

FULL PAPER

Open Access



# Vault-housed extensometers recorded a rapid initial pulse before precursory magma reservoir inflation related to the 2011 eruption of Shinmoe-dake, Japan

Ken'ichi Yamazaki<sup>1\*</sup> , Yusuke Yamashita<sup>1</sup> and Shintaro Komatsu<sup>2</sup>

## Abstract

Previous studies of the major eruption at Shinmoe-dake volcano, Japan, in January 2011 suggested that gradual injection of magma from a deep source into a shallow reservoir began in December 2009 and led to the major eruption. To investigate the initial phase of this injection event, we examined extensometer data from the Isa Observatory, ~ 18.5 km from the summit of Shinmoe-dake, and discovered a strain change event that spanned about 3 days in December 2009. The size of the strain change is comparable to those observed during each sub-Plinian eruption in 2011. The source of the rapid strain change appears to be deeper than the estimated location of the magma reservoir that directly supplied magma to the 2011 eruption sequence. These observations suggest that rapid injection of magma from the deep magmatic plumbing system in December 2009 triggered the continuous ascent of additional magma from depth, which in turn drove the climactic eruptions in January 2011. Extensometers also recorded two rapid strain change events of the same order of magnitude and with similar characteristics in December 2006 and August 2008; however, noticeable inflation of the edifice was not detected immediately following either event. This suggests that transient injection of magma into a shallow reservoir is not always followed immediately by a gradual recharge process.

**Keywords:** Shinmoe-dake 2011, Magma reservoir, Gradual inflation, Rapid inflation, Extensometer, Volcano monitoring, Strain, Magma intrusion

## Introduction

Most monitored volcanoes show detectible unrest before major eruptions. An unrest state is most clearly detectible in ground deformation (e.g., Nooner and Chadwick 2016; Morales Rivera et al. 2017), but can include changes in seismicity (e.g., Johnson et al. 2010) and migration of earthquake swarms (e.g., Nakada et al. 1999; Chiba and Shimizu 2018). These unrest states are potential precursors to major eruptions, although an eruption

does not always follow unrest (e.g., Moran et al. 2011). The transition from unrest to eruption has been studied at many volcanoes (e.g., Newhall and Hoblitt 2002), because unrest often leads to urgent improvements in monitoring. In contrast, transition from a quiescent state to unrest is less monitored and seldom studied, in part because there are fewer opportunities for observation.

This study focuses on Shinmoe-dake, one of the volcanic cones in the Kirishima volcanic group of southwest Japan. The 2011 eruption of Shinmoe-dake was its first major eruption in 52 years, although minor eruptions are common (e.g., in 1991 and 2010). The 2011 eruption sequence at Shinmoe-dake was characterized by three sub-Plinian eruptions, followed by magma effusion from

\*Correspondence: yamazaki.kenichi.4u@kyoto-u.ac.jp

<sup>1</sup> Miyazaki Observatory, Research Center for Earthquake Prediction, Disaster Prevention Research Institute, Kyoto University, 3884, Kaeda, Miyazaki 889-2161, Japan

Full list of author information is available at the end of the article

the summit crater, over a 6-day period spanning 26–31 January 2011 (Nakada et al. 2013). This activity was monitored using a dense geophysical network, and relevant data have been intensively studied (e.g., Kato and Yamasato 2013; Nakao et al. 2013; Ueda et al. 2013). One important finding, inferred from analysis of GNSS data, is that gradual inflation of the volcanic edifice began in late 2009 (Nakao et al. 2013); implying that the supply of magma began or accelerated at this time. Petrological studies suggest that the gradual inflation was driven by a continuous upward supply of high-temperature magma, from the deeper magmatic plumbing system to the shallow reservoir, which resulted in a major eruption through a turnover process (Tomiya et al. 2013). This scenario explains the transition from unrest to eruption; however, it remains unclear as to why a gradual supply of magma began or accelerated suddenly in late 2009. One way to answer this question is to search for geodetic signatures of the initial process that led to sustained magma injection.

An effective tool for observing small-scale geodetic phenomena is the vault-housed extensometer (also called a strainmeter). In some volcanoes, subtle ground deformation is observed prior to eruptions, as reported at Sakurajima, Japan (e.g., Kamo and Ishihara 1986; Ishihara 1990; Iguchi et al. 2008) and Piton de la Fournaise, Réunion, France (Peltier et al. 2006). Kyoto University maintains vault-housed extensometers at monitoring sites in southwest Japan (e.g., Harada et al. 2003), including Isa Observatory (ISA), ~18.5 km from the summit of Shinmoe-dake. Vault-housed extensometer data are easily distorted by meteorological conditions, such as rainfall (Kasahara et al. 1983) and temperature changes (Yamazaki 2013), which makes it difficult to observe strain changes on long timescales (>10 days). However, on timescales of hours to days, very small changes can be detected. Yamazaki et al. (2013) reported subtle changes in strain recorded by distal extensometers shortly before the 2011 Shinmoe-dake eruption, and related these changes to gas emission from the crater prior to the explosive eruptions.

To investigate the onset of gradual edifice inflation, we rechecked extensometer data from ISA and found a rapid strain change in late 2009. This paper reports the observations and describes an analysis of the source location, uniqueness (or non-uniqueness), and implications for magma resupply.

### Strain observations at ISA

The extensometer data that are the focus of the present report were recorded at ISA of Kyoto University (Fig. 1). ISA houses tunnels that extend in three directions: E1 (N37° W), E2 (N53° E), and E3 (N82° W). Each tunnel

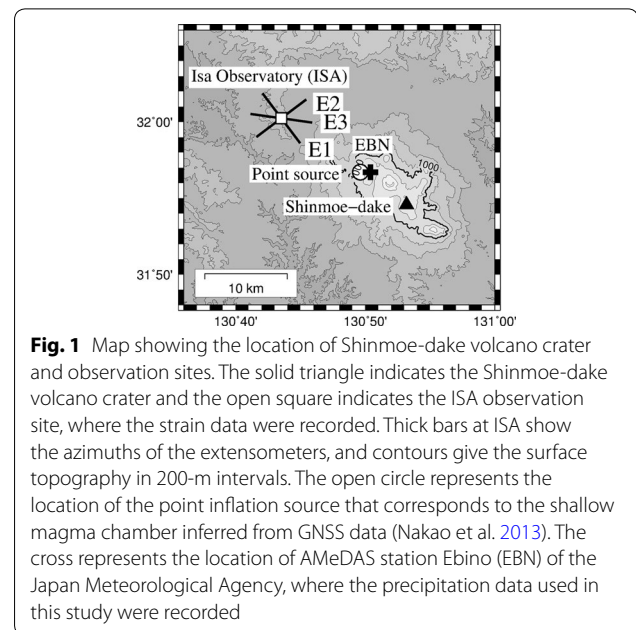


**Fig. 1** Map showing the location of Shinmoe-dake volcano crater and observation sites. The solid triangle indicates the Shinmoe-dake volcano crater and the open square indicates the ISA observation site, where the strain data were recorded. Thick bars at ISA show the azimuths of the extensometers, and contours give the surface topography in 200-m intervals. The open circle represents the location of the point inflation source that corresponds to the shallow magma chamber inferred from GNSS data (Nakao et al. 2013). The cross represents the location of AMeDAS station Ebino (EBN) of the Japan Meteorological Agency, where the precipitation data used in this study were recorded

houses an extensometer comprising a 30-m-long FeNi36 alloy rod (Fig. 2 of Yamazaki et al. 2013) for which the thermal expansion at room-temperature is empirically determined to be about  $10^{-6} \text{ } ^\circ\text{C}^{-1}$  (Yamazaki 2013). One end of each extensometer is fixed to the ground, and the other end is free. Displacement of the free end is measured using a differential transformer, and the amount of displacement is divided by the length of the rod to obtain the ground extension or contraction (strain) in the corresponding direction. The precision of strain measurement data at ISA is as good as  $1 \times 10^{-9}$ .

Shinmoe-dake is located ~18.5 km from ISA at an azimuth of S55.48° E (Fig. 1). The magma reservoir that supplied the 2011 eruption was estimated to be laterally offset from the summit (Nakao et al. 2013), but the azimuth from ISA to the shallow magma reservoir is approximately the same as that to the summit itself. The 18.5 km distance is large compared with monitoring stations for other volcanoes, such as Sakurajima, Japan (e.g., Kamo and Ishihara 1986); because of this separation, strain data recorded at ISA might be less sensitive to volumetric changes related to subsurface pressurized magma than at facilities located closer to their respective volcanoes. Nevertheless, distal extensometers at ISA are more sensitive to some types of subsurface volume changes than GNSS-based measurements, as demonstrated quantitatively by Yamazaki et al. (2013).

Figure 2 shows the strain record at ISA from January 2004 to December 2017. Daily precipitation data from the Ebino station (EBN; Fig. 1), provided by the Japan Meteorological Agency, are also shown. Note that

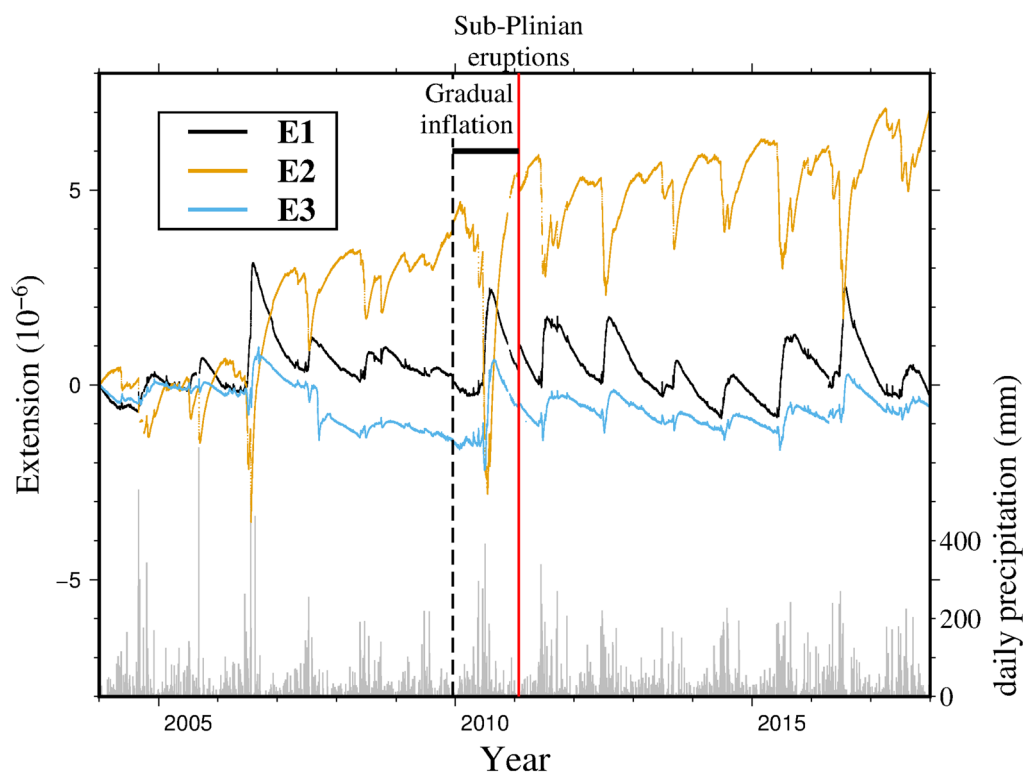


**Fig. 2** Strain change along the directions of instruments E1, E2, and E3, from the beginning of 2004 until the end of 2017. Daily precipitation at EBN is also shown (gray bar graph). The vertical red line marks the 2011 sub-Plinian eruptions. The vertical dashed line and thick horizontal bar indicate the onset and duration of the gradual inflation of the edifice, respectively (e.g., Nakao et al. 2013)

precipitation clearly affects the extensometers: during and immediately after heavy rain there is often extension in E1 and E3 and contraction in E2, followed by recovery (i.e., strain changes with opposite signs). Because of these effects, ground deformation cannot be quantified using the extensometers. Below, we analyze the extensometer data with consideration for the effect of rain.

### Strain changes at ISA coincident with the onset of edifice inflation

Details of the strain change at the beginning of inflation can be inferred from visual inspection of the time series. Figure 3 shows raw and detrended extensometer data, with daily precipitation data from EBN. A clear change in strain is recognized on each component during 15–17 December 2009. Before and during this change, little precipitation is observed; therefore, the observed strain change is unlikely to be caused by rain-related distortion. The strain change is characterized by extension on E2 and contraction on E1, which we expect when ground deformation is generated by a subsurface pressure source in the azimuthal direction of Shinmoe-dake. This observation suggests that rapid pressurization, on a time scale

of a few days, occurred beneath Shinmoe-dake at the beginning of the period of gradual inflation of the magma reservoir inferred from GNSS data (Nakao et al. 2013).

To quantify the strain changes of 15–17 December 2009, the linear trend must be removed from the original time series data. These trends were probably caused by heavy rains during the preceding summer and are unlikely to be related to volcanic deformation. Detrended time series are shown in Fig. 3b. From visual inspection, we estimate that the values of the strain changes in directions E1, E2, and E3 are  $-1.6 \pm 0.2$ ,  $+1.7 \pm 0.3$ , and  $-0.8 \pm 0.2$ , respectively, with units of  $10^{-7}$  strain. The strain changes are as large as those observed during each sub-Plinian eruption at Shinmoe-dake in January 2011 (Yamazaki et al. 2013). This suggests that the volume change during the December 2009 event was the same order of magnitude as previous eruptions that occurred during each sub-Plinian eruption.

If we assume that the strain change is generated by a subsurface spherical source in a homogeneous elastic isotropic half-space, the azimuth of the strain event relative to the observatory can be estimated using the ratio of strain changes in the three directions. If we further

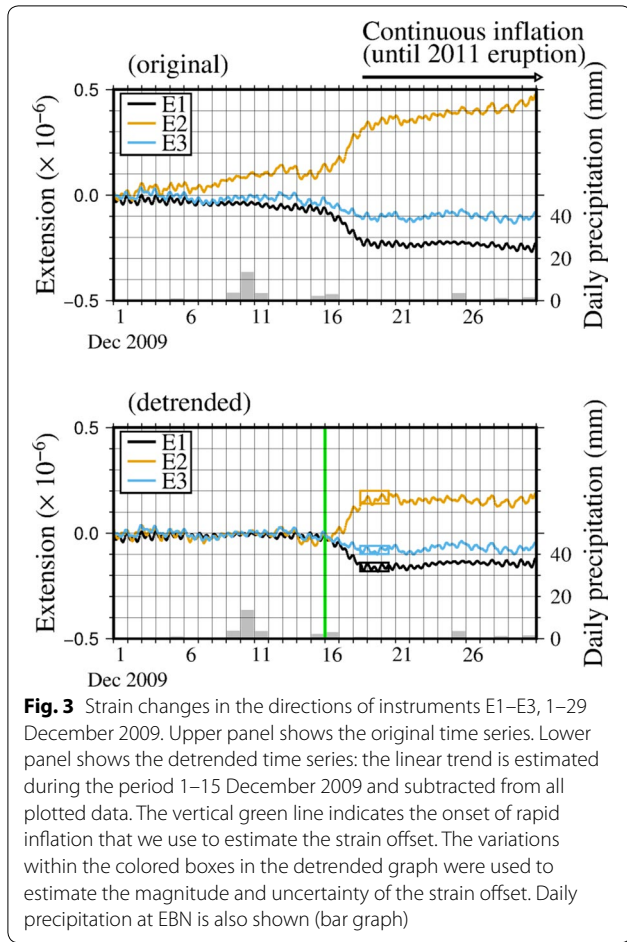


**Fig. 3** Strain changes in the directions of instruments E1–E3, 1–29 December 2009. Upper panel shows the original time series. Lower panel shows the detrended time series: the linear trend is estimated during the period 1–15 December 2009 and subtracted from all plotted data. The vertical green line indicates the onset of rapid inflation that we use to estimate the strain offset. The variations within the colored boxes in the detrended graph were used to estimate the magnitude and uncertainty of the strain offset. Daily precipitation at EBN is also shown (bar graph)

assume the spherical source can be approximated by a point, the equation for the ground deformation caused by this model has an analytical solution (Yamakawa 1955), with the displacement,  $d$ , given by

$$d(r) = (1 - \nu) \frac{\Delta V}{\pi} \frac{r}{(r^2 + h^2)^{3/2}} \quad (1)$$

where  $r$  and  $h$  are the distance from the epicenter and source depth, respectively (Fig. 4),  $\nu$  is Poisson’s ratio, and  $\Delta V$  is the volume change. By differentiating this equation, the change in strain is given by

$$f(r, D, I) = A(r, I) (1 - 3 \cos^2 D + \tan^2 I), \quad (2)$$

where  $D$  and  $I$  represent the azimuth and inclination relative to the extensometer, respectively (Fig. 4), and

$$A(r, I) = (1 - \nu) \frac{\Delta V}{\pi r^3} \frac{1}{(1 + \tan^2 I)^{5/2}}.$$

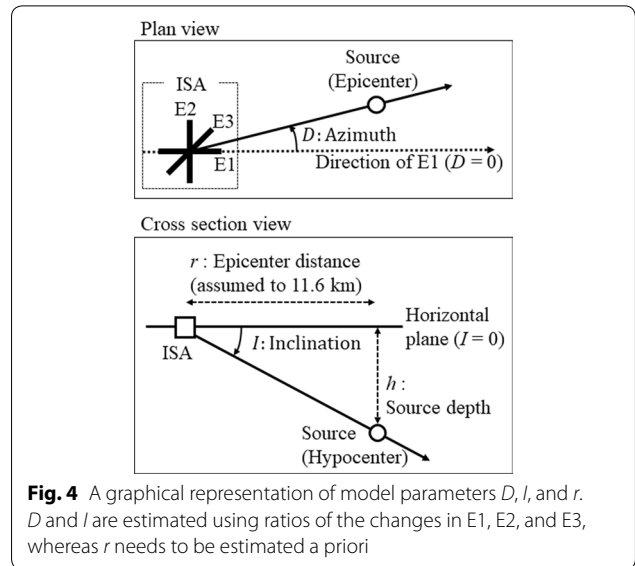


**Fig. 4** A graphical representation of model parameters  $D$ ,  $l$ , and  $r$ .  $D$  and  $l$  are estimated using ratios of the changes in E1, E2, and E3, whereas  $r$  needs to be estimated a priori

When the directions of E1 is set to  $D = D_1 = 0$  and the azimuth is measured in an anticlockwise sense, the relative azimuths of E2 and E3 are given by  $D_2 = D_1 + \pi/2$  and  $D_3 = D_1 + 3\pi/4$ , respectively. Consequently, the ratios E2/E1 and E3/E1 are given by  $f(r, D_1 + \pi/2, I)/f(r, D_1, I)$  and  $f(r, D_1 + 3\pi/4, I)/f(r, D_1, I)$ , respectively.

The estimated source direction of the rapid strain change in December 2009 is shown in Fig. 5, together with sources of strain changes observed during the

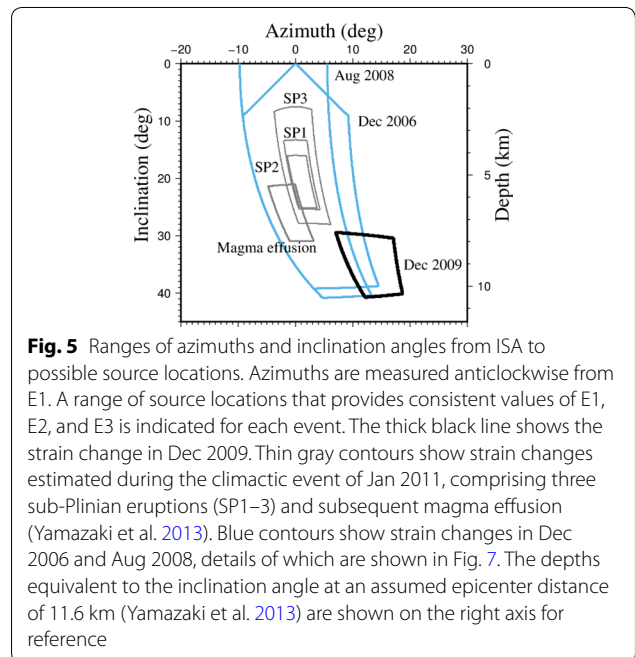


**Fig. 5** Ranges of azimuths and inclination angles from ISA to possible source locations. Azimuths are measured anticlockwise from E1. A range of source locations that provides consistent values of E1, E2, and E3 is indicated for each event. The thick black line shows the strain change in Dec 2009. Thin gray contours show strain changes estimated during the climactic event of Jan 2011, comprising three sub-Plinian eruptions (SP1–3) and subsequent magma effusion (Yamazaki et al. 2013). Blue contours show strain changes in Dec 2006 and Aug 2008, details of which are shown in Fig. 7. The depths equivalent to the inclination angle at an assumed epicenter distance of 11.6 km (Yamazaki et al. 2013) are shown on the right axis for reference

sub-Plinian eruptions and subsequent magma effusion in January 2011. Note that the depths of the two sources can only be compared using inclination angles (Fig. 4). If the depth of one source is greater than another, it will also have a larger inclination, unless the two sources are horizontally distant. Our results suggest that the rapid pressurization was deeper than the shallow magma reservoir that fueled the major eruption. Because a point source is a rough approximation of a magma reservoir, the absolute location may not be correct; however, the relative depths of the two events should be correct if the same point source model and dataset are used. This validates our conclusions regarding the relative depths and sizes of the sources.

The volume change that generated this inflation was large. The strain changes observed in December 2009 are as large as those observed during each sub-Plinian eruption in January 2011 (Yamazaki et al. 2013), suggesting that the volume change was the same order of magnitude as that of each sub-Plinian eruption, which is estimated to be  $1.0 \times 10^6 \text{ m}^3$  (Table 1 from Yamazaki et al. 2013). If the source of the December 2009 event is deeper than that of the sub-Plinian eruptions in 2011, then the December 2009 volume change would have been even greater. Assuming an epicenter distance of 11.6 km, a source depth of 8–10 km, and a Poisson's ratio of 0.25 gives a volume change of  $0.6 \times 10^6 \text{ m}^3$  to  $2.7 \times 10^6 \text{ m}^3$ .

### Other sizable strain changes at ISA

To check whether the strain change at ISA in December 2009 was a unique or recurring phenomenon, we examine the strain change rate from component E1 over the entire period for which site data acquired by the same instrumental system are available (Fig. 6). We set a threshold level for strain change rate of  $\pm 1.5 \times 10^{-9} \text{ day}^{-1}$ , which

is half the total strain change rate in December 2009. The times at which strain change rates exceed the threshold are considered to be prominent events of rapid strain change. Periods after heavy rainfall are ignored in this analysis because strain data in such periods are likely to be distorted.

In the obtained time series, there are seven anomalies in strain change rate in which values exceed the threshold (Fig. 6): four positive (i.e., extension of E1) and three negative (i.e., contraction of E1). Among the positive anomalies in strain change rate, three (2004, 2008, and 2013) occurred after significant precipitation and are therefore likely to reflect rainfall. Another positive anomaly in strain change rate in 2011 corresponds to the major eruption at Shinmoe-dake. In addition to the event in December 2009 (Fig. 3), negative anomalies in strain change rate are seen in December 2006 and August 2008. Extensometer data for these events are shown in Fig. 7.

The anomaly in December 2006 has the same characteristics as the event in December 2009: extension on component E2 and contraction on E1 and E3 (Fig. 7a). The anomaly in August 2008 also has the same characteristics, although each component returns to its original value after rain on 22 and 23 August (Fig. 7b). Their respective timings correspond to changes in observed volcanic activity at Shinmoe-dake: the first roughly corresponds to a subtle change in the GNSS baseline trend (Fig. 2 of Nakao et al. 2013); the second corresponds to the start of a period of phreatic eruptions (Fig. 5 of Nakada et al. 2013).

We now consider the strain changes in each direction from Fig. 7. During 2–6 December 2006, the estimated changes in components E1, E2, and E3 are  $-1.0 \pm 0.2$ ,  $+0.8 \pm 0.2$ , and  $-0.2 \pm 0.2$ , respectively, with units of  $10^{-7}$  strain (Fig. 7a). During 17–19 August 2008,

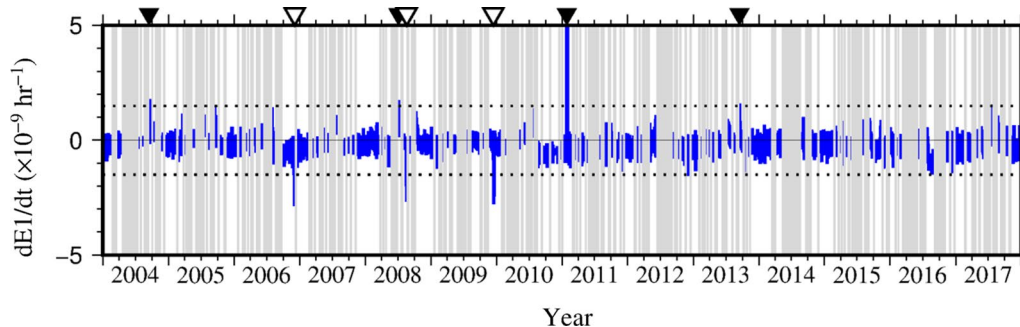


**Fig. 6** Strain change rate on component E1 at station ISA, 2004–2017. The strain change rate is defined as the time derivative of the 24-h moving average of the original time series. Gray shadows correspond to time periods in which significant precipitation ( $>40 \text{ mm/h}$ ) was observed in the previous week, which likely affects strain data. Open (positive) and solid (negative) inverted triangles indicate strain rates that exceed the threshold levels of  $1.5 \times 10^{-9} \text{ day}^{-1}$  (dotted lines). The threshold value is half the strain rate at the beginning of the edifice inflation that led to the major eruption in 2011

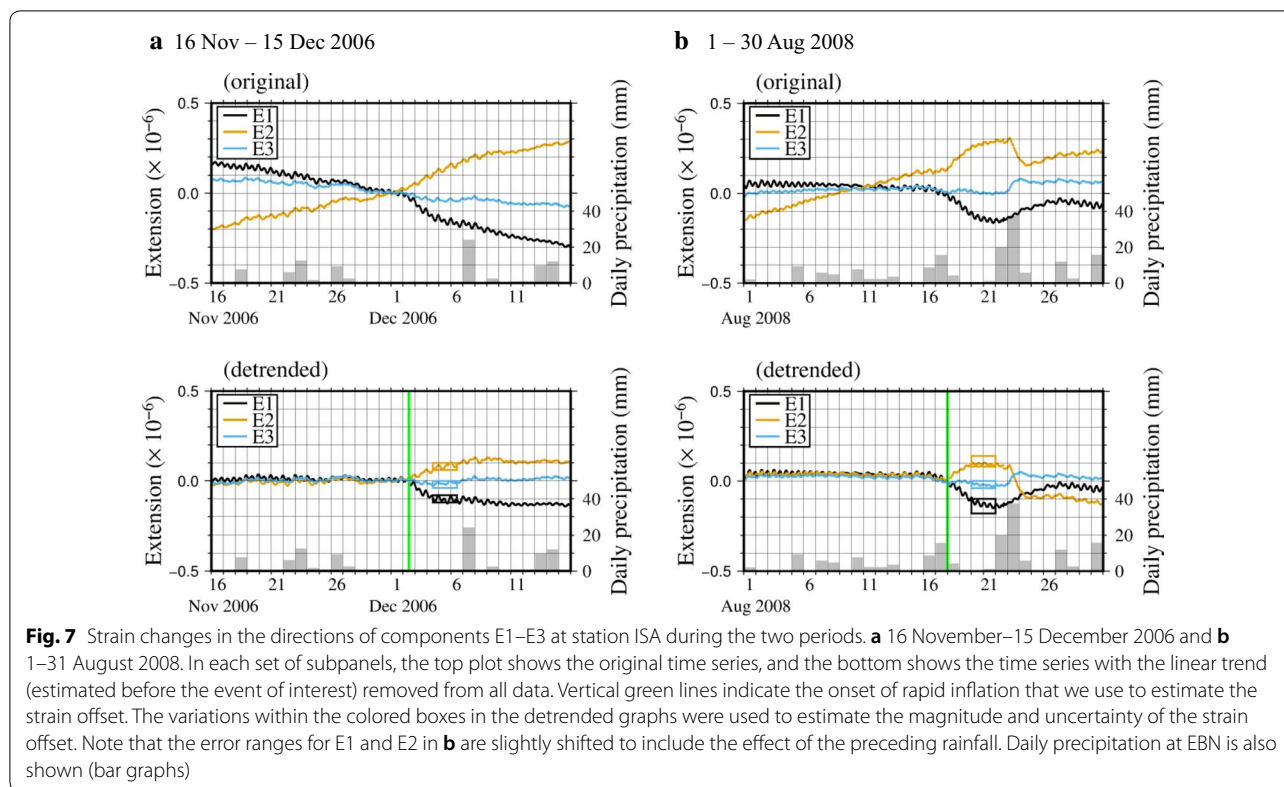


**Fig. 7** Strain changes in the directions of components E1–E3 at station ISA during the two periods. **a** 16 November–15 December 2006 and **b** 1–31 August 2008. In each set of subpanels, the top plot shows the original time series, and the bottom shows the time series with the linear trend (estimated before the event of interest) removed from all data. Vertical green lines indicate the onset of rapid inflation that we use to estimate the strain offset. The variations within the colored boxes in the detrended graphs were used to estimate the magnitude and uncertainty of the strain offset. Note that the error ranges for E1 and E2 in **b** are slightly shifted to include the effect of the preceding rainfall. Daily precipitation at EBN is also shown (bar graphs)

**Table 1** Changes in strain in each direction during each period

Period	E1 ( $\times 10^{-7}$ )	E2 ( $\times 10^{-7}$ )	E3 ( $\times 10^{-7}$ )
1–3 Dec 2006	$-1.0 \pm 0.2$	$0.8 \pm 0.2$	$-0.2 \pm 0.2$
17–19 Aug 2008	$-1.4 \pm 0.4$	$1.1 \pm 0.3$	$-0.2 \pm 0.2$
15–17 Dec 2009	$-1.6 \pm 0.2$	$1.7 \pm 0.3$	$-0.8 \pm 0.2$

the corresponding values are  $-1.4 \pm 0.4$ ,  $+1.1 \pm 0.3$ , and  $-0.2 \pm 0.2$ , respectively, with units of  $10^{-7}$  strain (Fig. 7b). These values, together with those during 15–17 December 2009, are listed in Table 1. Based on these values, the possible range of point source locations corresponding to each event is estimated (blue contours in Fig. 5). It is difficult to constrain the strain change rate more precisely because there are relatively large errors in the readings; hence, the estimated locations have large uncertainties. However, this confirms that the source locations of the 2006 and 2008 events overlap that of the December 2009 event.

**Discussion**

Petrological evidence suggests that eruption of stored magma is triggered by injection of new magma into a reservoir, presumably through dikes rising from depth (Suzuki et al. 2013; Tomiya et al. 2013). Basaltic replenishment at the beginning of the eruptive cycle triggers subsequent activity. Examples of eruptions with this inferred source process include the 1996 eruption of Karymsky Volcano in Kamchatka (Eichelberger and Izbekov 2000; Izbekov et al. 2004), the 1912 eruption of Katmai in Alaska (Eichelberger and Izbekov 2000), and the 1929 eruption of Hokkaido-Komagatake in Japan (Takeuchi and Nakamura 2001). In the case of the January 2011 Shinmoe-dake eruption, the volcanic processes leading to the eruption sequence were inferred from petrological and geodetic observations (Suzuki et al. 2013; Tomiya et al. 2013). GNSS time series show gradual edifice inflation before the main eruptions, but no pulse-like changes just before each eruption. This constraint leads to the interpretation that the final physical change before the eruption was a mixing process, which does not result in a volumetric change in the shallow magma reservoir (Tomiya et al. 2013).

The extensometer data presented here provide the first geophysical evidence of a rapid and large ( $\sim 10^{-7}$ ) strain change at the beginning of a period of gradual inflation

of a shallow reservoir that fed major eruptions. Weak signals that could indicate an injection pulse in December 2009 are present in the GNSS time series data (e.g., Figure 2 of Nakao et al. 2013), but extensometer data show their characteristics more clearly: 2–3 days in duration with a source that was deeper than the magma reservoir that fed the sub-Plinian eruptions. Moreover, the point source that generated this rapid inflation appears deeper than the magma reservoir that supplied the 2011 eruption sequence (Fig. 6). This implies that the ground deformation detected in the present work was not generated by the inflation of pre-existing magma in a reservoir, but rather by intrusion from depth. The rapid intrusion of fresh, hot basaltic magma at the onset of the magmatic inflation episode does not alter the petrologically derived scenario, but does provide additional constraints on the physical processes at the start of unrest, including the observed precursory gradual inflation.

In addition to an inflationary event in mid-December 2009, extensometers recorded several strain change events at other times with the same order of magnitudes and characteristics (Figs. 6, 7, Table 1). This means that a discrete, impulsive injection of magma is not a necessary or sufficient condition for triggering continuous magma injection from depth. Focusing on the sizes of inflation events observed from 2004 through 2017, the mid-December 2009 event is the largest in the raw records. Two other events, in August 2006 and December 2008, are relatively small and were not followed by sizable magma intrusions, although GNSS time series indicate a small change in strain rate around the beginning of December 2006 (Fig. 2 of Nakao et al. 2013). A possible explanation for these phenomena is that continuous injection of fresh magma into a shallower reservoir might be triggered only when the initial magma flux exceeds a threshold sufficient to open a new pathway from the deep magma system. Another possible explanation is that the pathway of magmas extending from depth to the magma reservoir is partially opened by each new intrusion. After three intrusions, the pathway opening might have become large enough to facilitate continuous upward magma flux. Although these scenarios could account for the volcanic processes related to the 2011 eruption sequence, they cannot be verified using the available geodetic data for this eruption sequence and other observations or physical considerations are necessary to confirm their validity.

To assess the frequency and size of rapid magma intrusions, comprehensive analysis of geodetic data is required. This cannot be done by extensometers alone because they do not correctly record strain change during and after heavy rainfall. In addition to previously installed sites, geodetic monitoring of Shinmoe-dake

using GNSS and tiltmeters has been improved (e.g., Ueda et al. 2013). Assuming the estimated volume changes and source depths correspond to rapid magma intrusion, ground displacements of several millimeters are expected for similar intrusion events in the future. These could be detected by GNSS, although the detailed temporal variations may be difficult to observe. Now that the time scale and approximate location of the rapid magma intrusion have been determined, a search for magma intrusion events is planned using GNSS and tiltmeter time series data via time series analysis, including matched-filter techniques (Gibbons and Ringdal 2006).

## Conclusions

Before the 2011 eruption of Shinmoe-dake volcano, Japan, at the beginning of precursory inflation of the volcanic edifice, a rapid change in strain was recorded by distal extensometers on a time scale of about 3 days. The size of the observed strain change is as large as that generated by the volcano's sub-Plinian eruptions. Assuming that the strain change is generated by a point source, the source location is estimated to be deeper than the shallow magma reservoir that fed the eruption itself. Rapid strain changes with similar characteristics were also recorded at least twice during 2004–2017 and relate to observed changes in eruptive activity.

## Abbreviations

ISA: Isa–Yoshimatsu observatory operated by Kyoto University; EBN: Ebino meteorological observation site operated by Japan Meteorological Agency.

## Acknowledgements

This work was motivated by discussions with Hiroaki Takahashi (Hokkaido University, Japan) and Koki Aizawa (Kyushu University, Japan). Observations at ISA are conducted by the staff of the Disaster Prevention Research Institute, Kyoto University, particularly by Masahiro Teraishi, Yasumi Sonoda, and Tetsuro Takayama. Constructive comments from Yosuke Aoki and an anonymous reviewer improved the contents and presentation of the manuscript. Figures were drawn using Generic Mapping Tools (Wessel and Smith 1998). Precipitation data from the Automated Meteorological Data Acquisition System (AMeDAS) dataset can be downloaded from the website of the Japan Meteorological Agency (in Japanese, url: <https://www.jma.go.jp/jp/amedas/>; last accessed: 20 January 2020).

## Authors' contributions

KY inspected the data, performed all analysis, and drafted the manuscript. YY contributed to the interpretation of results and data acquisition. SK contributed to the data acquisition and assisted in the inspection of data. All authors read and approved the final manuscript.

## Funding

This study was funded mainly by Kyoto University, and partially by the Ministry of Education, Culture, Sports, Science and Technology (MEXT) of Japan, under its Observation and Research Program for Prediction of Earthquakes and Volcanic Eruptions.

## Availability of data and materials

The datasets generated and analyzed during the current study are not publicly available due to the prior use rights of the data acquirer, but are available from the corresponding author on reasonable request.

**Ethics approval and consent to participate**

Not applicable.

**Consent for publication**

Not applicable.

**Competing interests**

The authors declare that they have no competing interests.

**Author details**

<sup>1</sup> Miyazaki Observatory, Research Center for Earthquake Prediction, Disaster Prevention Research Institute, Kyoto University, 3884, Kaeda, Miyazaki 889-2161, Japan. <sup>2</sup> Miyazaki Observatory, Division of Technical Affairs, Disaster Prevention Research Institute, Kyoto University, 3884, Kaeda, Miyazaki 889-2161, Japan.

Received: 3 March 2020 Accepted: 30 May 2020

Published online: 08 June 2020

**References**

- Chiba K, Shimizu H (2018) Spatial and temporal distributions of b-value in and around Shinmoe-dake, Kirishima volcano, Japan. *Earth Planets Space* 70:122. <https://doi.org/10.1186/s40623-018-0892-7>
- Eichelberger JC, Izbekov PE (2000) Eruption of andesite triggered by dyke injection: contrasting cases at Karymsky Volcano, Kamchatka and Mt Katmai, Alaska. *Philos Trans R Soc Lond A* 358:1465–1485. <https://doi.org/10.1098/rsta.2000.0599>
- Gibbons SJ, Ringdal F (2006) The detection of low magnitude seismic events using array-based waveform correlation. *Geophys J Int* 165:149–166
- Harada M, Furuzawa T, Teraishi M, Ohya F (2003) Temporal and spatial correlations of the strain field in tectonic active region, southern Kyusyu, Japan. *J Geodyn* 35:471–481. [https://doi.org/10.1016/S0264-3707\(03\)00008-5](https://doi.org/10.1016/S0264-3707(03)00008-5)
- Iguchi M, Yakiwara H, Tameguri T, Hendrasto M, Hirabayashi H (2008) Mechanism of explosive eruption revealed by geophysical observations at the Sakurajima, Suwanosejima and Semeru volcanoes. *J Volcanol Geotherm Res* 178:1–9
- Ishihara K (1990) Pressure sources and induced ground deformation associated with explosive eruptions at an andesitic volcano: Sakurajima volcano, Japan. In: Ryan M (ed) *Magma transport and storage*. Wiley, New York, pp 335–356
- Izbekov PE, Eichelberger JC, Boris V (2004) The 1996 eruption of Karymsky Volcano, Kamchatka: historical record of basaltic replenishment of an Andesite reservoir. *J Petrol* 45:2325–2345. <https://doi.org/10.1093/ptrology/egh059>
- Johnson JH, Prejean S, Savage MK, Townend J (2010) Anisotropy, repeating earthquakes, and seismicity associated with the 2008 eruption of Okmok volcano, Alaska. *J Geophys Res*. <https://doi.org/10.1029/2009jb006991>
- Kamo K, Ishihara K (1986) Precursor of summit eruption observed by water-tube tiltmeters and extensometers. *Annuals Disas Prev Res Inst Kyoto Univ.* 29(1):1–12 (in Japanese with English abstract)
- Kasahara M, Shichi R, Okada Y (1983) On the cause of long-period crustal movement. *Tectonophysics* 97(1–4):327–336
- Kato K, Yamasato H (2013) The 2011 eruptive activity of Shinmoedake volcano, Kirishimayama, Kyushu, Japan—overview of activity and volcanic alert level of the Japan Meteorological Agency. *Earth Planets Space* 65:489–504. <https://doi.org/10.5047/eps.2013.05.009>
- Morales Rivera AM, Amelung F, Mothes P, Hong S-H, Nocquet J-M, Jarrin P (2017) Ground deformation before the 2015 eruptions of Cotopaxi volcano detected by InSAR. *Geophys Res Lett* 44:6607–6615. <https://doi.org/10.1002/2017GL073720>
- Moran SS, Newhall C, Roman DC (2011) Failed magmatic eruptions: late-stage cessation of magma ascent. *Bull Volcanol* 73:115–122. <https://doi.org/10.1007/s00445-010-0444-x>
- Nakada S, Shimizu H, Ohta K (1999) Overview of the 1990–1995 eruption at Unzen Volcano. *J Volcanol Geotherm Res* 89:1–12. [https://doi.org/10.1016/S0377-0273\(98\)00118-8](https://doi.org/10.1016/S0377-0273(98)00118-8)
- Nakada S, Nagai M, Kaneko T, Suzuki Y, Maeno F (2013) The outline of the 2011 eruption at Shinmoe-dake (Kirishima), Japan. *Earth Planets Space* 65:475–488. <https://doi.org/10.5047/eps.2013.03.016>
- Nakao S, Morita Y, Yakiwara H, Oikawa J, Ueda H, Takahashi H, Ohta Y, Matsushima T, Iguchi M (2013) Volume change of the magma reservoir relating to the 2011 Kirishima Shinmoe-dake eruption—charging, discharging and recharging process inferred from GPS measurements. *Earth Planets Space* 65:505–515. <https://doi.org/10.5047/eps.2013.05.017>
- Newhall CG, Hoblitt RP (2002) Constructing event trees for volcanic crises. *Bull Volcanol* 64:3–20. <https://doi.org/10.1007/s004450100173>
- Nooner SL, Chadwick WW Jr (2016) Inflation-predictable behavior and co-eruption deformation at Axial Seamount. *Science* 354:1399–1403. <https://doi.org/10.1126/science.aah4666>
- Peltier A, Staudacher T, Catherine P, Ricard L-P, Kowalski P, Bachelery P (2006) Subtle precursors of volcanic eruptions at Piton de la Fournaise detected by extensometers. *Geophys Res Lett* 33:L06315
- Suzuki Y, Yasuda A, Hokanishi N, Kaneko T, Nakada S, Fujii T (2013) Syneruptive deep magma transfer and shallow magma remobilization during the 2011 eruption of Shinmoe-dake, Japan—constraints from melt inclusions and phase equilibria experiments. *J Volcanol Geotherm Res* 257:184–204
- Takeuchi S, Nakamura M (2001) Role of precursory less-viscous mixed magma in the eruption of phenocryst-rich magma: evidence from the Hokkaido-Komagatake 1929 eruption. *Bull Volcanol* 63:365–376. <https://doi.org/10.1007/s004450100151>
- Tomiya A, Miyagi I, Saito G, Geshi N (2013) Short time scales of magma-mixing processes prior to the 2011 eruption of Shinmoedake volcano, Kirishima volcanic group, Japan. *Bull Volcanol* 75:750. <https://doi.org/10.1007/s00445-013-0750-1>
- Ueda H, Kozono T, Fujita E, Hohno Y, Nagai M, Miyagi Y, Tanada T (2013) Crustal deformation associated with the 2011 Shinmoe-dake eruption as observed by tiltmeters and GPS. *Earth Planets Space* 65:517–525. <https://doi.org/10.5047/eps.2013.03.001>
- Wessel P, Smith WHF (1998) New, improved version of generic mapping tools released. *EOS Trans AGU* 79:579. <https://doi.org/10.1029/98EO00426>
- Yamakawa N (1955) On the strain produced in a semi-infinite elastic solid by an interior source of stress, Zishin 2nd series. *J Seismol Soc Jpn* 8:84–98
- Yamazaki K (2013) An attempt to correct strain data measured with vault-housed extensometers under variations in temperature. *Tectonophysics* 599:89–96. <https://doi.org/10.1016/j.tecto.2013.04.001>
- Yamazaki K, Teraishi M, Ishihara K, Komatsu S, Kato K (2013) Subtle changes in strain prior to sub-Plinian eruptions recorded by vault-housed extensometers during the 2011 activity at Shinmoe-dake, Kirishima volcano, Japan. *Earth Planets Space* 65:1491–1499. <https://doi.org/10.5047/eps.2013.09.005>

**Publisher's Note**

Springer Nature remains neutral with regard to jurisdictional claims in published maps and institutional affiliations.